A Coupled OpenFOAM-GEMS Framework for Simulating Fission Product Release from Molten Salt Reactors

Dowon Lee[a], Juhyeong Lee[a], JinHo Song[a], Sung Joong Kim[*a,b]
[a]*Department of Nuclear Engineering, Hanyang University*
222 Wangsimni-ro, Seongdong-gu, Seoul 04763, Republic of Korea
[b]*Institute of Nano Science and Technology, Hanyang University*
222 Wangsimni-ro, Seongdong-gu, Seoul 04763, Republic of Korea
[*]*Corresponding author: sungjkim@hanyang.ac.kr*

Keywords : Molten salt reactor, OpenFOAM, GEMS, Fission product release, Mechanistic source term

1. Introduction

Molten Salt Reactors (MSRs) have been recognized as promising candidates for next-generation nuclear power systems owing to their inherent safety features, fuel flexibility, and potential for high thermal efficiency. These advantages make MSRs attractive alternatives to conventional Light Water Reactors (LWRs). As the development and deployment of MSRs progress, the necessity of establishing appropriate regulatory frameworks has become increasingly evident.

However, due to the distinct safety characteristics and fission product behavior of MSRs, existing regulatory guidelines such as TID-14844 and NUREG-1465 are not directly applicable [1-2].

To address these challenges, the U.S. Nuclear Regulatory Commission (NRC) introduced the Mechanistic Source Term (MST) approach, as outlined in documents such as SECY-93-092 [3]. The MST enables physics-based evaluations of source terms under accident conditions. It supports a more reliable understanding of fission product release, transport and retention, which is crucial for advanced reactor licensing and safety analysis.

In support of MST evaluations for MSRs, the Paul Scherrer Institute (PSI) developed cGEMS, a coupled code system that integrates MELCOR and GEMS [4]. MELCOR is a engineering-level, lumped parameter code for severe accident analysis, and GEMS is a thermodynamic equilibrium solver. Although cGEMS contributes MST-based source term analysis, its MELCOR component lacks the capability to simulate local thermofluid phenomena, which are closely linked to the behavior of fission products during accident conditions.

To overcome the limitation of cGEMS, a new coupled framework integrating OpenFOAM, a computational fluid dynamics (CFD) platform, with GEMS has been developed. The OpenFOAM-GEMS framework enables high-fidelity simulations of radionuclide behavior during accident scenarios based on detailed thermohydraulic analyses. In this study, the coupling methodology, modeling approach, and verification case of the framework are described.

2. Model Description and Coupling Methodology

This section introduces the implementation details of a coupled analysis tool developed for MST source term evaluations in MSRs. The framework integrates OpenFOAM, GEMS, and a mass release model. Key components such as the initialization of species data, vapor pressure fitting, surface mass transfer modeling, decay heat feedback, and isotope tracking are described in the following subsections.

2.1 Governing equations for Thermofluid Analysis

The thermofluid behavior of molten salt under accident conditions is modeled using OpenFOAM. The framework is designed to be flexible, allowing users to choose an appropriate OpenFOAM solver based on the characteristic of the target scenario, including flow type and compressibility.

The governing equations are based on the conservation laws for mass, momentum, and energy, as shown in Equations (1) – (3):

$$\frac{\partial \rho}{\partial t} + \nabla \cdot (\rho \boldsymbol{u}) = 0 \tag{1}$$

$$\frac{\partial (\rho \boldsymbol{u})}{\partial t} + \nabla(\rho \boldsymbol{u} \otimes \boldsymbol{u}) = -\nabla p + \nabla \cdot (\tau + \tau_{RANS}) + \rho \boldsymbol{g} \tag{2}$$

$$\frac{\partial (\rho h)}{\partial t} + \nabla \cdot (\rho h \boldsymbol{u}) = \nabla \cdot (k \nabla T) + Q \tag{3}$$

where ρ is fluid density, $\boldsymbol{u}$ is velocity, p is pressure, τ is the viscous stress tensor, τ_{RANS} is the Reynolds stress tensor, $\boldsymbol{g}$ is gravitational acceleration, h is specific enthalpy, T is temperature, k is thermal conductivity, and Q is the volumetric heat source, which includes decay heat contributions from radioactive isotopes.

After solving the governing equations at each time step, the surface temperature and pressure are extracted. Specifically, the surface temperature and pressure refer to the values of the computational cells adjacent to the free surface boundary. These values serve as the primary input for the GEMS calculation (Section 2.2) and the mass release model (Section 2.3).

2.2 Thermodynamic Equilibrium Calculation

The thermodynamic equilibrium state of the molten salt at the gas-liquid interface is calculated using the GEMS. The code determines the most stable phase and species distribution of a chemical system by minimizing its total Gibbs free energy, subject to the constraints of mass balance.

The calculation process begins with a comprehensive thermodynamic database. This database is populated with the necessary thermodynamic properties for all relevant elements, compounds, and phases expected in the system. The key properties include standard molar enthalpy of formation (ΔH_f°), standard molar entropy (S°), and heat capacity ($C_p(T)$) for each species.

At each time step, the analysis requires two primary inputs. First, the surface temperature and pressure are provided by the OpenFOAM solutions, as described in Section 2.1. Second, the initial element composition of the molten salt, derived from fuel burnup calculations, defines the total molar amount of each element in the system. The output of the GEMS calculation is the equilibrium distribution of all chemically stable compounds.

The discrete Gibbs free energy data is post-processed into continuous vapor pressure functions for efficient use in the transient simulation. For each key species, the vapor pressure (P_{vap}) is calculated from the Gibbs free energy of vaporization (ΔG) and temperature (T) using the thermodynamic relation in Equation (4):

$$P_{vap} = \exp\left(-\frac{\Delta G}{RT}\right) \tag{4}$$

This calculation, performed across a wide temperature range, generates a large set of (T, P_{vap}) data points based on the GEMS thermodynamics database. The data points are fitted to the Antoine equation, shown as Equation (5):

$$\log_{10}(P_{vap}) = A - \frac{B}{T + C} \tag{5}$$

where A, B, and C are the Antoine coefficients to be determined. The fitting is specifically focused on the 800 K to 1600 K temperature range, which is of primary interest for MSR accident scenarios. The coefficients were optimized to ensure the Normalized Root Mean Square Error (NRMSE) remained below 5 %. This entire procedure is performed as a pre-processing step using a Python script to generate a reliable set of Antoine coefficients before the main coupled simulation begins.

2.3 Surface Mass Release Model

The data exchange time step, which must be kept short to satisfy the CFD solver's stability requirements, is not necessarily sufficient for the system to reach the full thermodynamic equilibrium predicted by GEMS. Relying solely on the thermodynamic limit could therefore lead to an overestimation of the species release.

To address this potential limitation, a dual-limit approach is implemented. The framework calculates not only the thermodynamic limit (Section 2.2) but also a kinetic limit based on mass transfer theory. The final release rate is then determined by selecting the smaller of these two values to ensure a more physically realistic estimation of the release.

The kinetic limit is calculated using a Diffusion-Limited Evaporation Model [5]. This model assumes that the rate of evaporation is not only driven by the vapor pressure at the surface but also limited by the rate at which the evaporated molecules can diffuse away from the surface through the bulk gas. The molar flux due to the kinetic limitation, φ_{kin} (mol/m^2·s), is calculated as Equation (6):

$$\varphi_{kin} = \frac{k_g}{RT_{surf}}\left(P_{vap} - P_{\infty}\right) \tag{6}$$

where k_g is the mass transfer coefficient (m/s), R is the universal gas constant, T_{surf} is the surface temperature, P_{vap} is the equilibrium vapor pressure at the surface (from the Antoine fit) and P_{∞} is the partial pressure of the species in the bulk gas far from interface.

The mass transfer coefficient is defined by the binary diffusivity of the species, D_{AB}, and an assumed stagnant boundary layer thickness, δ, over which diffusion is the dominant transport mechanism ($k_g = D_{AB}/\delta$) . The binary diffusivity, D_{AB}, which quantifies how quickly one gas species (A) diffuses through another gas species (B) , is calculated from first principle using the Chapman-Enskog theory. This theory requires fundamental molecular properties as input, the Lennard-Jones parameters: the collision diameter (σ) and the potential well depth (ϵ/k) , which represent the molecular size and intermolecular attraction forces, respectively.

The instantaneous molar flux is integrated over the surface area (A_{surf}) and the discrete data exchange time step (Δt) to calculate the total number of moles released, N_{kin}, as shown in Equation (7):

$$N_{kin} = \varphi_{kin} \cdot A_{surf} \cdot \Delta t \tag{7}$$

Finally, at each time step, the code compares the potential evaporated moles from thermodynamic limit (GEMS results), N_{thermo}, with the kinetic limit, N_{kin}. The actual number of moles released and tracked in the framework, $N_{release}$ is the minimum of these two values:

$$N_{release} = \min(N_{thermo}, N_{release}) \tag{8}$$

This ensures that the calculated release is both thermodynamically possible and physically realistic given the constraints of mass transport.

2.4 Isotope Tracking and Decay heat Model

To accurately capture the thermal behavior of molten salt during an accident, the framework incorporates an isotope tracking and decay heat model. The decay heat model simulates the heat generated by radioactive fission products and provides critical feedback to the thermofluid simulation.

The release of specific isotopes is determined through a two-step process. First, the total molar release of each chemical element is determined by decomposing the released chemical compounds into their constituent elements based on their stoichiometry. Next, the loss of individual isotopes is calculated based on an isotopic ratio assumption, which posits that the isotopes of a given element are released in direct proportion to their existing molar ratio within the molten salt.

The calculated loss for each isotope is then subtracted from the condensed phase inventory, and added to the gas phase inventory. It is important to note that in the current single-phase simulation approach, this gas phase inventory is a tracked quantity used for source term accounting, and the model does not simulate the further transport of these species within the gas domain.

Furthermore, the model accounts for natural radioactive decay. Within each time step (ΔT), the inventory of each nuclide (N_i) is also updated using the exponential decay law, as shown in Equation (9):

$$N_i(t + \Delta t) = N_i(t) \exp(-\lambda_i \Delta t) \tag{9}$$

where λ_i is the specific decay constant for the isotope provided as input.

The updated inventory is critical for the subsequent time step calculations. The new gas phase inventory determines the partial pressure (P_∞) used in the mass release model (Equation 6). Simultaneously, the total heat generation, Q_{tot}, is computed from the updated condensed phase inventory. The calculation is a summation over all relevant radionuclides, as shown in Equation (10):

$$Q_{tot} = \Sigma_i N_{i.cond} \cdot q_i \tag{10}$$

where, $N_{i,cond}$ is the molar amount of isotope i in the condensed phase and q_i is its specific molar decay heat (W/mol), a value derived from the ENDF/B-VII.0 database. The calculated total decay heat, Q_{tot} (in W), is directly applied to the thermofluid simulation as heat source term, Q, in the energy conservation equation (Equation 3) via the fvOptions framework. This creates a fully coupled feedback loop between the source term evolution and the thermal-hydraulic behavior of the system.

2.5 Overview of the Coupled Framework

Section 2.5 provides a comprehensive overview of how the individual models described previously-thermofluid analysis (Section 2.1), thermodynamic equilibrium (Section 2.2), mass release (Section 2.3), and isotope tracking (Section 2.4)- are integrated and interact within the coupled framework. The goal is to create a physically realistic simulation where the thermofluid behavior and source term evolution are dynamically linked.

The overall coupling mechanism operates on a time-stepped basis, as shown in the flowchart in Figure 1. At each time step, the simulation proceeds in the following sequence:

1. The OpenFOAM solver calculates the fluid dynamics and heat transfer equations to provide the surface temperature and pressure.
2. Surface temperature, pressure and current isotopic inventory are passed to GEMS to determine the thermodynamic equilibrium state.
3. The thermodynamic limit and kinetic limit for mass release are calculated. The final molar release for the time step is determined by taking the minimum of these two values.
4. The isotope tracking model updates the inventories of both the condensed and gas phases based on the calculated release.
5. The new condensed phase inventory is used to calculate the total decay heat, and the value is fed back as a source term into OpenFOAM energy equation for the next time step.

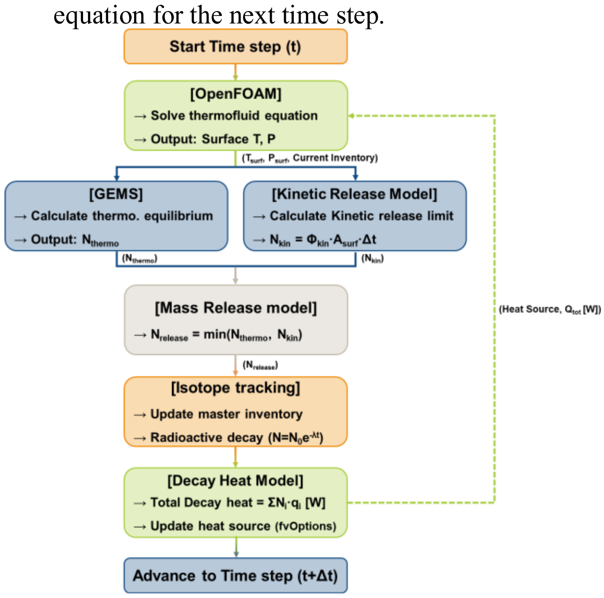

Fig. 1. Flowchart of the coupled OpenFOAM-GEMS framework for source term analysis

The main control logic for this framework is written in C++. Communication with the GEMS solver is handled directly via its Application Programming Interface (API), while feedback to the OpenFOAM solver is managed through scripted modification of input files. The OpenFOAM-GEMS integrated structure ensures a self-consistent analysis where the thermofluid behavior and source term evolution are dynamically coupled.

3. Case study and Results

3.1 Problem Description and Simulation Setup

To demonstrate the capability of the coupled OpenFOAM-GEMS framework, this study analyzes a simplified post-accident scenario based on the Passive

Molten Salt Fast Reactor (PMFR), for which detailed fuel burnup data is available. The analysis assumes a simple pool-type geometry representing a complete spill of the molten salt onto the floor. The geometry and computational mesh used for the scenario are shown in Figure 2.The dimensions of the computational domain were determined based on the total fuel salt volume of the PMFR. The mesh was constructed with 100, 5, and 60 cells in the x, y, and z directions.

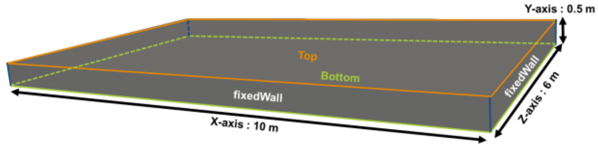

Fig. 2. Schematic of simulated geometry

The numerical schemes used for the OpenFOAM simulation are summarized in Table 1. The boundary conditions for the analysis, which include a fixed pressure of 1 atm at the gas-liquid interface, are detailed in Table 2. To investigate the impact of different thermal conditions on the evaporation behavior, 3 distinct cases (Case 1 to Case 3) were simulated by varying these boundary conditions as specified in the table. Furthermore, two different initial temperatures were set: 923.15 K for Case 1 and 2, and 1173.15 K for Case 3.

Table 1: Major parameters for OpenFOAM calculation

Parameters	Values
Simulation	
Solver	buoyantPimpleFoam
Turbulence model	k-epsilon model
Time step	5 s
Iteration and Discretization	
Iteration algorithm	PIMPLE (Pressure-Velocity coupling algorithm)
Smoother	symGaussSeidel
Time term	Euler
Gradient term	Gauss linear
Interpolation	Linear
Radiation Model	
Model	fvDOM

Table 2: Boundary conditions for each case

Boundary conditions	Values	
	Case 1 & 3	Case 2
Temperature boundary conditions		
Top Bottom	externalWallHeatFlux Temperature	zeroGradient
fixedWall	zeroGradient	
Velocity boundary conditions		
Top Bottom fixedWall	noSlip	
Pressure boundary condition		
Top	fixedFluxPressure (1 atm)	
Bottom fixedWall	prghTotalPressure	

The initial composition of the molten salt was based on a 14,000 day fuel burnup calculation for the PMFR, performed using the Serpent 2.2.1 code. The detailed isotopic inventory from the calculation was provided as input to the isotope tracking and decay heat models. For the GEMS calculation, the total molar amount of each element was summed from the isotopic data and used as the primary chemical input, as summarized in Table 3.

The bulk gas phase was assumed to be pure nitrogen (N_2). Based on a representative containment volume of 2000 m^3, the total molar of nitrogen was set to 89,875 mol. This value is used to determine the partial pressure of released species and as a key parameter in the kinetic release model. The small amount of argon (Ar) listed in Table 3 was included solely to enhance the numerical convergence stability of the GEMS calculation and does not affect the mass release model.

The GEMS thermodynamic database was constructed with 145 chemical compounds across gas, liquid, and solid phases. Based on a preliminary analysis of vapor pressures, the results presented in Section 3.2 will focus on 12 key species that are expected to have a significant impact on the total release: $BaCl_2$, BaI_2, $CeCl_3$, CsCl, CsI, KCl, $LaCl_3$, NaCl, $PuCl_3$, $SrCl_2$, UCl_3, and UCl_4.

Table 3: Initial elemental composition for GEMS calculation

Element	Symbol	Molar amount (mol)
Argon	Ar	0.0005
Barium	Ba	1607.35
Cerium	Ce	2171.06
Chlorine	Cl	1.00e+06
Cesium	Cs	760.133
Iodine	I	189.707
Potassium	K	117740
Lanthanum	La	1150.34
Nitrogen	N	89875
Sodium	Na	249709
Palladium	Pd	833.77
Plutonium	Pu	6311.65
Rhodium	Rh	633.361
Ruthenium	Ru	2455.87
Samarium	Sm	739.02
Strontium	Sr	1191.98
Tellurium	Te	459.145
Uranium	U	189148

3.2 Results and Discussion

Simulations for the 3 cases defined in Section 3.1 were performed for a total of 2,000 seconds. The results of this transient analysis are presented and discussed below, focusing on the overall thermal behavior, decay heat feedback, and the detailed speciation of the released source term.

Figure 3 shows the transient behavior of the molten salt surface temperature (dashed lines) and the total moles of evaporated gas (solid lines) for Cases 1, 2, and 3. In Cases 1 and 3, heat is removed from the system via conduction through the bottom boundary and a combination of convection and radiation from the top surface. As the external heat removal rate is greater than the internal decay heat generation, the surface temperature shows a continuous decrease. Conversely, Case 2, with its adiabatic boundaries, shows a steady temperature increase. This is driven by a natural circulation loop within the pool: the volumetric decay heat warms the bulk salt, reducing its density and causing it to rise. This circulation effectively transports the internally generated heat to the surface.

A key observation occurs at approximately 1000 seconds, where the temperature of Case 2 surpasses that of Case 3. Despite the temperature crossover, the total evaporated gas moles of Case 2 do not overtake those of Case 3. This demonstrates a critical aspect of the model: at the short time steps used in the simulation, the mass release is not solely governed by the thermodynamic limit. Instead, the kinetic limit, constrained by physical mass transport, becomes the dominant rate-limiting factor, preventing an immediate surge in evaporation even as the temperature becomes favorable.

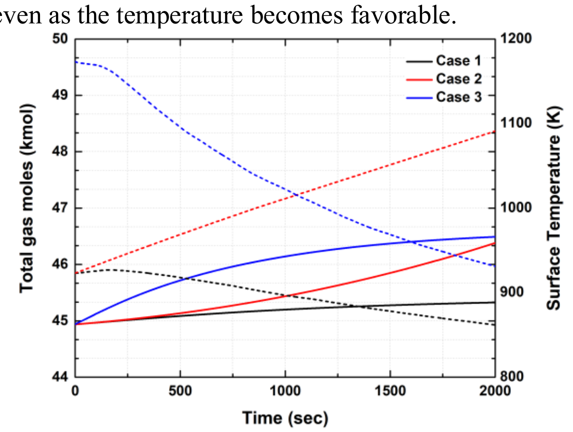

Fig. 3. Evolution of surface temperature (dashed lines) and cumulative gas moles (solid lines) over time for each case

The evolution of the total decay heat for each case is presented in Figure 4. The decay heat shows a nearly identical, steady decrease across all cases. This is primarily because the decay is governed by the exponential decay law (Equation 9), which is independent of the system's thermal conditions. However, the impact of nuclide release on the total decay heat appears minimal, primarily because Tellurium-129, which accounts for approximately 43.5% of the initial decay heat, has a very low volatility and was not observed to evaporate in any of the simulated cases. Consequently, the primary heat source remained within the condensed phase throughout the simulations.

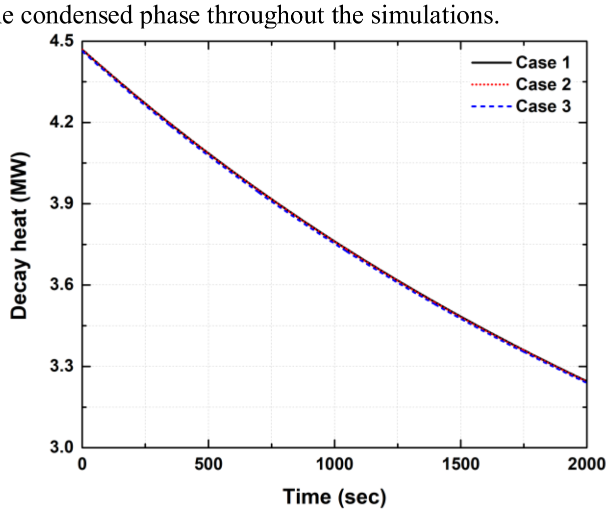

Fig. 4. Evolution of total decay heat over time for each case

Figure 5 illustrates the cumulative released mass of the 12 key chemical species for Case 1, 2, and 3, respectively. In all cases, UCl_4 is the most significantly released species due to its high vapor pressure, followed by other volatile chlorides such as CsCl, KCl, and NaCl.

The results clearly show the temperature dependency of evaporation for certain species. For example, the release of NaCl in Case 2 accelerates significantly as the temperature rises above 1050 K. Similarly, BaI_2, which has a low vapor pressure, shows negligible release in the low-temperature Case 1 where the driving force ($P_{vap} - P_{\infty}$) is minimal. However, in the higher-temperature Cases 2 and 3, its release becomes observable.

It is also noted that in Cases 1 and 3, where the temperature decreases, the cumulative released mass of the species does not decrease. This is a limitation of the current model, as a condensation model has not yet been implemented and is planned as future work.

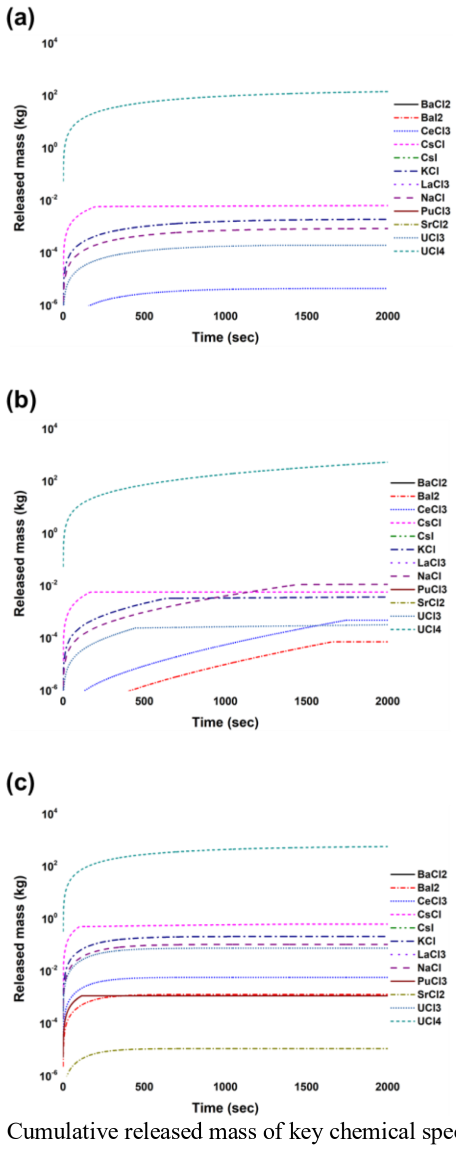

Fig. 5. Cumulative released mass of key chemical species over time for (a) Case 1, (b) Case 2, and (c) Case 3

3. Case study and Results

This study focused on the development and verification of a coupled simulation framework for MST analysis of MSR accident scenarios. The study involved integrating the OpenFOAM CFD solver with the GEMS thermodynamic code. The developed framework features a dual-limit (thermodynamic and kinetic) mass release model and a fully coupled isotope tracking and decay heat feedback mechanism. Key findings from the analysis of a simplified scenario include:

- ✓ The simulation results demonstrated that the kinetic limit, governed by mass transport, can be more restrictive than the thermodynamic limit, preventing a direct correlation between surface temperature and the evaporation rate, especially at short time steps.
- ✓ The total decay heat evolution was found to be largely independent of the nuclide release. This was because the primary heat-generating isotope (Te-129) exhibited very low volatility and remained in the condensed phase across all simulated cases.
- ✓ The chemical speciation of released source term was shown to be highly dependent on temperature, While UCl_4 was the dominant release species, the evaporation of other compounds like NaCl, BaI_2 was significant only above specific temperature thresholds.
- ✓ The framework successfully demonstrated the fully coupled feedback loop where the release of nuclides updated the isotopic inventory, which in turn affected the decay heat source term fed back into thermofluid simulation.

This study provides a more physically realistic tool for MSR source term analysis compared to system-level code. Future research will focus on enhancing the model's capabilities by implementing a condensation model to simulate the re-deposition of evaporated species. Furthermore, the framework will be applied to more realistic accident scenarios that explicitly model the dynamic spreading and flow of the molten salt during the initial spill phase.

Acknowledgements

This work was supported by the Human Resources Development of the Korea Institute of Energy Technology Evaluation and Planning (KETEP) grant funded by the Korea government Ministry of Knowledge Economy (RS-2024-00439210) and by Korea Foundation Of Nuclear Safety (KoFONS) using the financial resource granted by the RS-2025-02312295.

REFERENCES

[1] TID-14844, "Calculation of Distance Factors for Power and Test Reactor Sites", US AEC, 1962.
[2] NUREG-1465, "Accident Source Terms for Light Water Nuclear Power Plants", US NRC, 1995.
[3] NRC, "Issues Pertaining to the Advanced Reactor (PRISM, MHTGR, and PIUS) and CANDU 3 Designs and their Relationship to Current Regulatory Requirements," U.S. Nuclear Regulatory Commission SECY-93-092, 1993.
[4] Nichenko, S., Kalilainen, J., & Lind, T. (2022). MSR simulation with cGEMS: Fission product release and aerosol formation. Journal of Nuclear Engineering, 3(1), 105-116.
[5] Lewis, W. K., & Whitman, W. G. (1924). Principles of Gas Absorption. Industrial & Engineering Chemistry, 16(12), 1215–1220.